

A Porous 4d–4f Heterometallic Coordination Polymer: Synthesis, Crystal Structure and Physical Properties

Guang-Xiang Liu,*^[a] Xin-Long Li,^[a] Xiao-Chun Zha,^[a] Chun-You Zhang,^[a] Yan Wang,^[a] and Xiao-Ming Ren^[a]

Keywords: Heterometallic coordination polymer; Porous materials; Silver; Lanthanum; Gas adsorption

Abstract. A 4d–4f heterometallic coordination polymer, $[\text{AgLa}(\text{pydc})_2] \cdot 3\text{H}_2\text{O}$ (**1**) (H_2pydc = pyridine-3,4-dicarboxylic acid), has been synthesized under hydrothermal conditions, and further characterized by elemental analysis, IR spectroscopy, thermogravimetric analysis and single-crystal X-ray diffraction. Complex **1** features a three-dimensional (3D) framework containing one-dimensional (1D) channels occupied by free water molecules, which is constructed from

1D inorganic heterometallic chains and linear pydc linkers. To the best of our knowledge, complex **1** represents a rare example of 3D open-framework 4d–4f heterometallic coordination polymer. Moreover, after removal of the water molecules from complex **1**, the remaining material has high thermal stability and good adsorption behavior towards nitrogen gas.

Introduction

In the past two decades, great interest has been focused on the rapidly expanding field of the construction of novel functional metal-organic frameworks (MOFs) owing to their variety of intriguing architectures and topologies and their potential applications in magnetism, electric conductivity, gas adsorption, heterogeneous catalysis, nonlinear optics and fluorescent materials.^[1–12] Consequently, a variety of MOFs have been reported. However, much work on MOFs has been focusing on the design of lanthanide or transition homometallic system, whereas the chemistry towards heterometallic MOFs has attracted much less attention. Recently, some lanthanide–transition heterometallic complexes have been successfully obtained from spontaneous assembly of mixed metal ions and ligands containing hybrid donor atoms, such as cyanide,^[13] carbonyl,^[14] pyridine-carboxylate ligand,^[15] amino acids^[16,17] and so on. The assembly of three-dimensional (3D) heterometallic complexes, however, is still a challenge due to the variable and versatile coordination numbers of the lanthanide ions, their low stereochemical preference and also because of competitive reactions between lanthanide and transition metals coordinated to the same organic ligands. As is well-known, the lanthanides have a strong tendency to coordinate to O-donor atoms to form lanthanide-carboxylate coordination polymers,^[18] and compared to the Ln^{III} ions, the transition metal easily bonds to the N-donor atoms.^[19] Thus, if a ligand

containing both N-donor and O-donor atoms and the transition metal could be introduced to link the lanthanide–carboxylate subunits successfully, the novel heterometallic coordination polymers may be obtained through the recognition of the metal ions and their coordinating atoms.^[20]

On the other hand, great interest in Ln –Ag heterometallic complexes has recently focused on the nicotinic acid or isonicotinic acid.^[21–25] Compared with these two N-heterocyclic acids, pyridine-3,4-dicarboxylic acid (H_2pydc) can show richer coordination modes due to its two carboxylate groups, accordingly, it is an excellent candidate for the construction of metal organic frameworks. Although the synthesis of the monometallic coordination polymers based on H_2pydc ligand has become widespread over the recent years,^[26–31] investigations on heterometallic coordination polymers containing pydc^{2-} has not been extensively explored until now.^[32] In this paper, we chose pyridine-3,4-dicarboxylate as a bifunctional bridging ligand, which has oxygen and nitrogen donor atoms that can act as potential linkers between the lanthanide and the silver atoms. Herein, we report on the synthesis, crystal structure, thermal stability and nitrogen gas adsorption of a novel 4d–4f heterometallic coordination polymer, $[\text{AgLa}(\text{pydc})_2] \cdot 3\text{H}_2\text{O}$ (**1**).

Experimental Section

Materials and General Methods

All reagents commercially available were of reagent grade and used without further purification. Solvents were purified according to the standard methods. Elemental analyses were determined using a Vario EL III elemental analyzer. IR spectra were recorded in the 4000–400 cm^{-1} region using KBr pellets with a Nicolet AVATAR-360 spectrometer. Thermal gravimetric analyses (TGA) were performed with a Netzsch STA-409PC instrument in flowing N_2 with a heating rate of 10 $^{\circ}\text{C} \cdot \text{min}^{-1}$. Powder X-ray diffraction patterns (PXRD) were meas-

* Dr. G.-X. Liu
Fax: +86-556-5500090
E-Mail: njuliugx@gmail.com

[a] Anhui Key Laboratory of Functional Coordination Compounds
School of Chemistry and Chemical Engineering
Anqing Normal University
Anqing 246003, P. R. China

ured on a RigakuD/maxrA rotating anode X-ray diffractometer with graphite monochromatic Cu- K_{α} ($\lambda = 1.5418 \text{ \AA}$) radiation at room temperature. Nitrogen sorption experiments were carried out on a Belsorp-max volumetric gas sorption instrument. The sample was dried by using the “outgas” function of the surface area analyzer for 12 h at 200 °C to remove the solvents in the channels.

Preparation of Complex [AgLa(pydc)₂]·3H₂O (1)

A mixture of La₂O₃ (0.1 mmol, 65.0 mg), AgNO₃ (0.2 mmol, 34.0 mg), pyridine-3,4-dicarboxylic acid (0.4 mmol, 66.8 mg) and water (15 mL) was stirred for 30 min in air. Thereafter, the mixture was sealed in a 25 mL Teflon reactor and was kept under autogenous pressure at 180 °C for 7 days. Colorless block crystals were filtered off, washed with distilled water, and dried in air (yield: 65 % based on La). The as-synthesized material is insoluble in water and common organic solvents. C₁₄H₁₂N₂O₁₁AgLa: C 26.65; H 1.92; N 4.44; found: C 26.60; H 2.00; N 4.41 %. IR (KBr pellet): 3453 (m), 1622 (s), 1571 (s), 1476 (m), 1385 (s), 1162 (w), 1091 (w), 893 (w), 846 (m), 715 (m), 670 (w), 541(w) cm⁻¹.

X-ray Crystallography

The crystallographic data collections for complex **1** was carried out with a Bruker Smart Apex II CCD with graphite-monochromated Mo- K_{α} radiation ($\lambda = 0.71073 \text{ \AA}$) at 293(2) K using the ω -scan technique. The data were integrated by using the SAINT program,^[33] which also did the intensities corrected for Lorentz and polarization effect. An empirical absorption correction was applied using the SADABS program.^[34] The structures were solved by direct methods using the program SHELXS-97 and all non-hydrogen atoms were refined anisotropically on F^2 by the full-matrix least-squares technique using the SHELXL-97 crystallographic software package.^[35,36] The hydrogen atoms were generated geometrically except for water molecules. Hydrogen atoms of water molecules were located from difference Fourier maps and refined freely keeping the O–H bond lengths constrained to ~0.85 Å with the DFIX command. All calculations were performed on a personal computer with the SHELXL-97 crystallographic software package.^[36] The details of the crystal parameters, data collection and refinement for **1** are summarized in Table 1. Selected bond lengths and angles with their estimated standard deviations for **1** are shown in Table 2. Crystallographic data (excluding structure factors) for the structures reported in this paper have been deposited with the Cambridge Crystallographic Data Center as supplementary publication No. CCDC-813454. Copies of the data can be obtained free of charge on application to CCDC, 12 Union Road, Cambridge CB2 1EZ, UK [Fax: +44-1223-336-033; E-Mail: deposit@ccdc.cam.ac.uk].

Results and Discussion

The single-crystal X-ray analysis reveals complex **1** crystallizes in the triclinic space group $P\bar{1}$ and exhibits a novel 3D heterometallic coordination framework. As illustrated in Figure 1, there are one unique La^{III} ion, one Ag^I ion, two crystallographically unique pydc²⁻ anions and three lattice water molecules in the asymmetric unit. Each La^{III} ion is coordinated by nine oxygen atoms from six pydc²⁻ ligands in a distorted monocapped square antiprism geometry. The distances of La–O bonds range from 2.460(7) to 2.693(8) Å, similar to those in other La^{III} carboxylate complexes.^[37–39] The O–La–O bond

Table 1. Crystal Data and Refinement Results for Complex **1**.

	1
Empirical formula	C ₁₄ H ₁₂ N ₂ O ₁₁ AgLa
Molecular mass /g·mol ⁻¹	631.04
Color of crystal	Colorless
Crystal dimensions /mm	0.24 × 0.20 × 0.18
Temperature /K	293(2)
Lattice dimensions	
<i>a</i> /Å	7.445(5)
<i>b</i> /Å	10.617(7)
<i>c</i> /Å	11.720(8)
α /°	101.816(8)
β /°	100.422(7)
γ /°	97.006(8)
Unit cell volume /Å ³	879.5(10)
Crystal system	Triclinic
Space group	$P\bar{1}$ (No. 2)
<i>Z</i>	2
μ (Mo- K_{α}) /mm ⁻¹	3.576
<i>D</i> (calcd.) /g·cm ⁻³	2.383
Radiation type	Mo- K_{α}
<i>F</i> (000)	604
Limits of data collection /°	2.36 ≤ θ ≤ 25.10
Total reflections	5802
Unique reflections, parameters	3049, 262
No. with <i>I</i> > 2σ(<i>I</i>)	2303
<i>R</i> ₁ indices [<i>I</i> > 2σ(<i>I</i>)]	0.0672
<i>wR</i> ₂ indices	0.1643
Goodness of fit	1.020
Min/max peak (final diff. map) /e·Å ⁻³	-2.462 / 3.549

a) $R_1 = \sum |F_o| - |F_c| / \sum |F_o|$. b) $wR_2 = [\sum w(|F_o|^2 - |F_c|^2) / \sum w(F_o)^2]^{1/2}$, $w = 1 / [\sigma^2(F_o^2) + (aP)^2 + bP]$. $P = (F_o^2 + 2F_c^2)/3$.

Table 2. Selected bond lengths /Å and angles /° for complex **1**.

Ag(1)–N(1)	2.188(10)	La(1)–O(6)	2.561(9)
Ag(1)–N(2)#1	2.189(10)	La(1)–O(8)#2	2.584(7)
La(1)–O(4)#2	2.460(7)	La(1)–O(2)	2.596(8)
La(1)–O(5)#3	2.494(7)	La(1)–O(5)	2.677(7)
La(1)–O(8)#3	2.499(8)	La(1)–O(1)	2.693(8)
La(1)–O(3)#3	2.523(7)		
N(1)–Ag(1)–N(2)#1	145.8(4)	O(3)#3–La(1)–O(2)	137.8(3)
O(4)#2–La(1)–O(5)#3	123.0(3)	O(6)–La(1)–O(2)	126.9(3)
O(4)#2–La(1)–O(8)#3	71.8(3)	O(8)#2–La(1)–O(2)	144.8(3)
O(5)#3–La(1)–O(8)#3	70.7(2)	O(4)#2–La(1)–O(5)	148.3(2)
O(4)#2–La(1)–O(3)#3	137.4(2)	O(5)#3–La(1)–O(5)	68.5(3)
O(5)#3–La(1)–O(3)#3	67.1(2)	O(8)#3–La(1)–O(5)	135.5(2)
O(8)#3–La(1)–O(3)#3	74.8(3)	O(3)#3–La(1)–O(5)	73.7(2)
O(4)#2–La(1)–O(6)	122.7(3)	O(6)–La(1)–O(5)	49.8(2)
O(5)#3–La(1)–O(6)	113.3(3)	O(8)#2–La(1)–O(5)	121.0(2)
O(8)#3–La(1)–O(6)	142.3(3)	O(2)–La(1)–O(5)	92.2(2)
O(3)#3–La(1)–O(6)	73.3(3)	O(4)#2–La(1)–O(1)	80.2(2)
O(4)#2–La(1)–O(8)#2	76.7(3)	O(5)#3–La(1)–O(1)	101.0(2)
O(5)#3–La(1)–O(8)#2	129.5(2)	O(8)#3–La(1)–O(1)	137.8(3)
O(8)#3–La(1)–O(8)#2	74.4(3)	O(3)#3–La(1)–O(1)	141.8(3)
O(3)#3–La(1)–O(8)#2	69.3(2)	O(6)–La(1)–O(1)	79.7(3)
O(6)–La(1)–O(8)#2	76.0(3)	O(8)#2–La(1)–O(1)	129.2(2)
O(4)#2–La(1)–O(2)	68.3(3)	O(2)–La(1)–O(1)	49.3(3)
O(5)#3–La(1)–O(2)	70.7(3)	O(5)–La(1)–O(1)	68.2(2)
O(8)#3–La(1)–O(2)	90.5(3)		

Symmetry codes, #1 $x + 1, y + 1, z + 1$; #2 $x - 1, y, z$; #3 $-x + 1, -y + 1, -z$.

angles range from 49.3(3) to 148.3(2) $^{\circ}$. As far as the Ag^I ion is concerned, it exhibits a trigonal arrangement and is coordinated by two nitrogen atoms from two different pydc ligands (Ag–N, 2.188(10) and 2.189(10) Å) and an oxygen atom from one carboxylate (Ag–O, 2.627(10) Å). The N–Ag–O(N) bond angles are in the range 96.12(3)–145.78(4) $^{\circ}$.

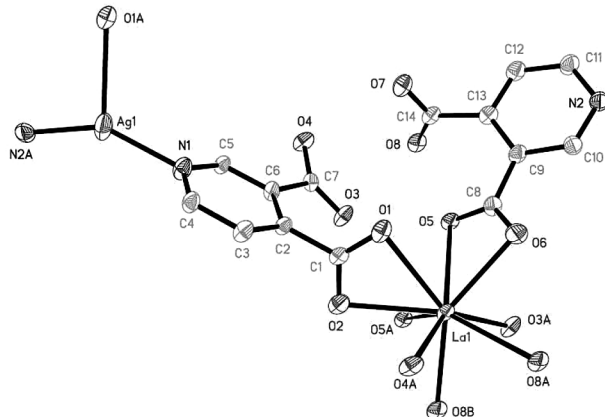
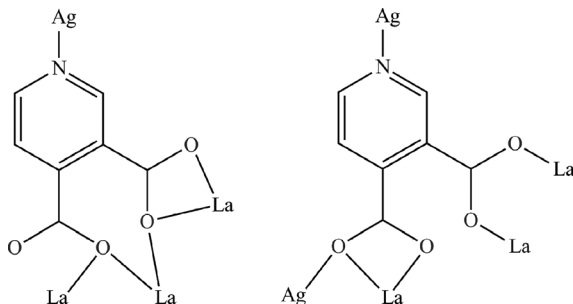


Figure 1. ORTEP drawing of complex **1** showing Ag^I and La^{III} coordination environment with thermal ellipsoids at 30 % probability.

It is interesting that two unique pydc²⁻ ligands exhibit two kinds of coordination modes as depicted in Scheme 1: one coordinated to three La^{III} ions and two Ag^I ions, the other bonded to three La^{III} ions and one Ag^I ion. On the basis of such coordination modes of pydc²⁻ ligands and the characteristics of lanthanide ions with the affinity of oxygen donors, 1D chain with La–O–La connectivity is built up from the edge-sharing La^{III} polyhedra along the *a* axis, and the distances between adjacent La^{III} ions in one chain are 4.049(3) and 4.277(3) Å. This analogous arrangement of inorganic chain can be found in homometallic lanthanide–carboxylate frameworks. However, the most important aspect is that this arrangement provides active oxygen atoms to construct a 1D inorganic heterometallic chain (Figure 2), in which the Ag^I atoms are anchored to the La–carboxylate chain through coordination bonds. That is, the 1D inorganic heterometallic chain can be regarded as the assembly of Ag^I atoms and inorganic chain with La–O–La connectivity through carboxylate oxygen atoms. Such a type of construction fashion is unusual in the system of lanthanide heterometallic coordination polymers.



Scheme 1. Coordination modes of the pydc²⁻ ligand in **1**.

The most striking feature of **1** is that each inorganic heterometallic subunit is linked to four neighboring subunits by

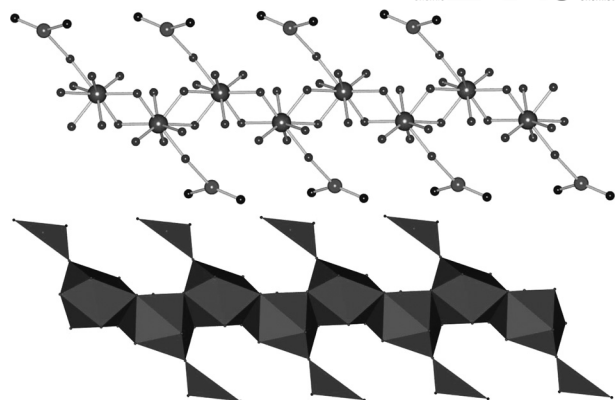


Figure 2. Perspective view of the 1D inorganic heterometallic chain in **1**: (top) ball-and-stick representation and (bottom) polyhedra representation. Carbon and hydrogen atoms are omitted for clarity.

pydc²⁻ linkers along both *b* and *c* directions, generating a 3D coordination framework (Figure 3). Due to the little hindrance of the pydc²⁻ ligand, the 1D rhombic channels are occupied by free water molecules. These channels have approximate dimensions of 8.682 × 12.411 Å. A π–π interaction exists between the pyridine rings of pydc²⁻ ligands, resulting in double-layer channel walls, and the closest C···C and C···N contacts between neighboring pyridine rings are 3.572(3) and 3.605(3) Å, respectively. Moreover, free water molecules have hydrogen-bonding interaction with pydc²⁻ ligands in the host framework, which to some degree improve the stability of the heterometallic framework. After the removal of these free water molecules, PLATON^[40] calculations show that the volume of the effective void is 25.2 % of the unit-cell volumes. Up to now, only a few 3D 4d–4f heterometallic coordination polymers have been reported. To the best of our knowledge, complex **1** is a rare 3D 4d–4f heterometallic coordination polymer with open framework structure.

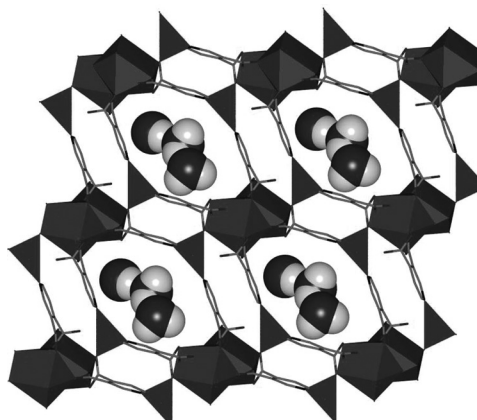


Figure 3. Perspective view of the 3D coordination framework of **1** with lattice water molecules occupying the 1D channels along the *a* axis.

Thermal Analysis

The thermal stability of **1** was determined by thermogravimetric analysis (TGA) (Figure 4). TGA was performed at a heating rate of $10\text{ }^{\circ}\text{C}\cdot\text{min}^{-1}$ with single-crystal samples of **1**. Thermal analysis of the complex shows that there are two obvious steps of weight loss in the temperature range of $20\text{--}800\text{ }^{\circ}\text{C}$. The first step, occurring between $60\text{ and }120\text{ }^{\circ}\text{C}$, is attributed to the loss of three free water molecules per formula (observed weight loss, 8.90%; calcd, 8.55%). The weight is almost unchanged in the temperature range of $120\text{--}410\text{ }^{\circ}\text{C}$. The sharp weight loss above $410\text{ }^{\circ}\text{C}$ corresponds to the decomposition of complex **1** and the remaining weight of 44.79% is the metal oxide. This means that complex **1** is stable up to the high temperature of $410\text{ }^{\circ}\text{C}$.

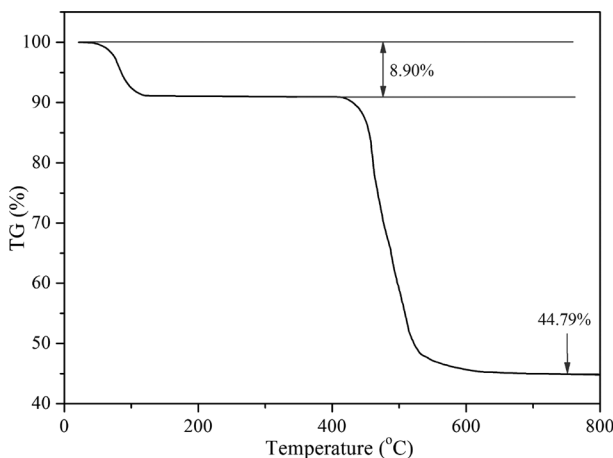


Figure 4. TGA curve of complex **1**.

PXRD and Gas Adsorption Property

The purity of complex **1** is confirmed by powder X-ray diffraction (PXRD) analysis, in which the experimental PXRD pattern is in well agreement with the one obtained from the stimulated PXRD based on the single crystal samples at room temperature (Figure 5). To verify whether the framework of **1** can be sustained after the removal of the solvent molecules, activated PXRD patterns were measured (Figure 5). The framework of **1** still has good crystallinity without solvent water molecules, and thus gas sorption of **1** was investigated. Before gas adsorption tests, the activation for removing the water molecules from the pores by heating under a vacuum is a required pretreatment and the as-synthesized crystal samples of **1** were heated at an optimized temperature of $200\text{ }^{\circ}\text{C}$ for 12 h.

Gas storage study was performed on sample of complex **1** after removing the free water molecules. N_2 adsorption for complex **1** at 77 K (Figure 6) shows reversible type I isotherms characteristic of microporous materials with uptake of $166\text{ cm}^3\cdot\text{g}^{-1}$ and calculated BET surface area of $517\text{ m}^2\cdot\text{g}^{-1}$. The gas sorption isotherms show hysteresis between the adsorption-desorption curves, which may be attributed to the intercrystalline voids.^[41]

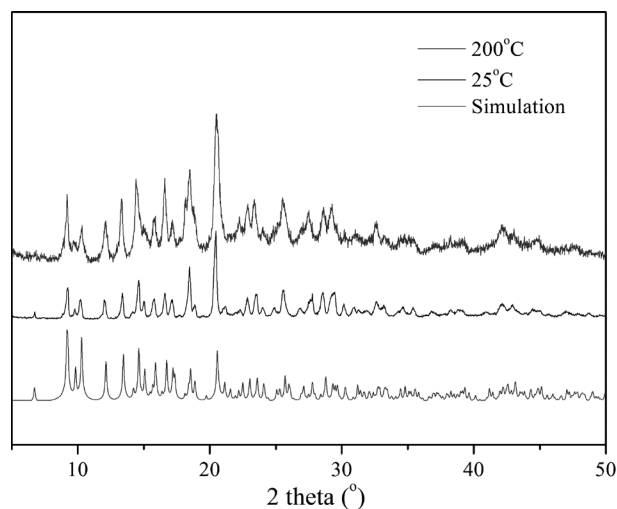


Figure 5. X-ray power diffraction profiles of complex **1** after heat treatment in air. Data were collected on (a) theoretic simulation from the single crystal data; (b) the as-synthesized crystal obtained directly from the reaction; (c) the same crystal after heating it to $200\text{ }^{\circ}\text{C}$ for 12 h.

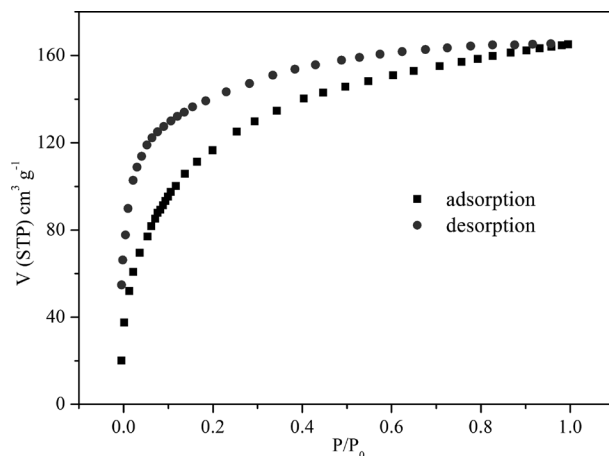


Figure 6. N_2 adsorption isotherms (77 K) for complex **1**.

Conclusions

In summary, we have successfully synthesized a novel 4d–4f coordination polymer based on pyridine-3,4-dicarboxylate, which shows a three-dimensional (3D) coordination framework, containing one-dimensional (1D) channels occupied by free water molecules and represents a rare example of 3D open-framework 4d–4f heterothallic coordination polymer. Moreover, after removal of the water molecules from complex **1**, the remaining material has high thermal stability and good adsorption behavior towards nitrogen gas, which could be useful for providing functional pores.

Acknowledgement

This work was supported by the National Natural Science Foundation of China (Nos. 20971004, 20901004), the Key Project of Chinese Min-

istry of Education (No. 210102) and the Natural Science Foundation of Anhui Province (No. 11040606M45).

References

- [1] M. Shibasaki, N. Yoshikawa, *Chem. Rev.* **2002**, *102*, 2187.
- [2] J. Inanaga, H. Furuno, T. Hayano, *Chem. Rev.* **2002**, *102*, 2211.
- [3] C. E. Plečnik, S. M. Liu, S. G. Shore, *Acc. Chem. Res.* **2003**, *36*, 499.
- [4] R. E. P. Winpenny, *Chem. Soc. Rev.* **1998**, *27*, 447.
- [5] S. J. A. Pope, B. J. Coe, S. Faulkner, E. V. Bichenkova, X. Yu, K. T. Douglas, *J. Am. Chem. Soc.* **2004**, *126*, 9490.
- [6] A. Bencini, C. Benelli, A. Caneschi, R. L. Carlin, A. Dei, D. Gatteschi, *J. Am. Chem. Soc.* **1985**, *107*, 8128.
- [7] W. F. Yeung, T. C. Lau, X. Y. Wang, S. Gao, L. Szeto, W. T. Wong, *Inorg. Chem.* **2006**, *45*, 6756.
- [8] B. Q. Ma, S. Gao, G. Su, G. X. Xu, *Angew. Chem.* **2001**, *113*, 448; *Angew. Chem. Int. Ed.* **2001**, *40*, 434.
- [9] S. M. Liu, E. A. Meyers, S. G. Shore, *Angew. Chem.* **2002**, *114*, 3761; *Angew. Chem. Int. Ed.* **2002**, *41*, 3609.
- [10] A. D. Cutland-Van Noord, J. W. Kampf, V. L. Pecoraro, *Angew. Chem.* **2002**, *114*, 4861; *Angew. Chem. Int. Ed.* **2002**, *41*, 4667.
- [11] C. M. Zaleski, E. C. Depperman, J. W. Kampf, M. L. Kirk, V. L. Pecoraro, *Angew. Chem.* **2004**, *116*, 4002; *Angew. Chem. Int. Ed.* **2004**, *43*, 3912.
- [12] Y. F. Zhou, M. C. Hong, X. T. Wu, *Chem. Commun.* **2006**, 135.
- [13] D. W. Knoepfel, S. G. Shore, *Inorg. Chem.* **1996**, *35*, 5328.
- [14] J. M. Boncella, R. A. Anderson, *Inorg. Chem.* **1984**, *23*, 432.
- [15] Y. C. Liang, R. Cao, W. P. Su, M. C. Hong, W. J. Zhang, *Angew. Chem.* **2000**, *112*, 3442; *Angew. Chem. Int. Ed.* **2000**, *39*, 3304.
- [16] J. J. Zhang, S. Q. Xia, T. L. Sheng, S. M. Hu, G. Leibeling, F. Meyer, X. T. Wu, S. C. Xiang, R. B. Fu, *Chem. Commun.* **2004**, 1186.
- [17] J. J. Zhang, T. L. Sheng, S. M. Hu, S. Q. Xia, G. Leibeling, F. Meyer, Z. Y. Fu, L. Chen, R. B. Fu, X. T. Wu, *Chem. Eur. J.* **2004**, *10*, 3963.
- [18] Y. P. Ren, L. S. Long, B. W. Mao, Y. Z. Yuan, R. B. Huang, L. S. Zheng, *Angew. Chem.* **2003**, *115*, 550; *Angew. Chem. Int. Ed.* **2003**, *42*, 532.
- [19] W. Shi, X. Y. Chen, Y. N. Zhao, B. Zhao, P. Cheng, A. Yu, H. B. Song, H. G. Wang, D. Z. Liao, S. P. Yan, Z. H. Jiang, *Chem. Eur. J.* **2005**, *11*, 5031.
- [20] X. J. Gu, D. F. Xue, *Inorg. Chem.* **2006**, *45*, 9257.
- [21] X. J. Gu, D. F. Xue, *CrystEngComm* **2007**, *9*, 471.
- [22] Y. C. Qiu, H. G. Liu, Y. Ling, H. Deng, R. H. Zeng, G. Y. Zhou, M. Zeller, *Inorg. Chem. Commun.* **2007**, *10*, 1399.
- [23] Y. B. Dong, J. Y. Cheng, J. P. Ma, R. Q. Huang, *Cryst. Growth Des.* **2005**, *5*, 585.
- [24] X. J. Gu, D. F. Xue, *Cryst. Growth Des.* **2006**, *6*, 2551.
- [25] X. J. Gu, D. F. Xue, *Cryst. Growth Des.* **2007**, *7*, 1726.
- [26] S. Q. Xia, S. M. Hu, J. C. Dai, X. T. Wu, J. J. Zhang, Z. Y. Fu, W. X. Du, *Inorg. Chem. Commun.* **2004**, *7*, 51.
- [27] C. Qin, X. L. Wang, E. B. Wang, L. Xu, *Inorg. Chim. Acta* **2006**, *359*, 417.
- [28] X. D. Zhu, S. Y. Gao, Y. F. Li, H. X. Yang, G. L. Li, B. Xu, R. Cao, *J. Solid State Chem.* **2009**, *182*, 421.
- [29] H. H. Song, Y. J. Li, *Inorg. Chim. Acta* **2008**, *361*, 1421.
- [30] X. L. Wang, C. Qin, E. B. Wang, L. Xu, Z. M. Su, *J. Mol. Struct.* **2006**, *796*, 172.
- [31] D. Ang, G. B. Deacon, P. C. Junk, D. R. Turner, *Polyhedron* **2007**, *26*, 385.
- [32] X. J. Gu, D. F. Xue, *CrystEngComm* **2007**, *9*, 471.
- [33] SAINT, Version 6.02a; Bruker AXS Inc.: Madison, WI, **2002**.
- [34] G. M. Sheldrick, *SADABS*, Program for Bruker Area Detector Absorption Correction, University of Göttingen, Göttingen, Germany, **1997**.
- [35] G. M. Sheldrick, *SHELXS-97*, Program for Crystal Structure Solution, University of Göttingen, Göttingen, Germany, **1997**.
- [36] G. M. Sheldrick, *SHELXL-97*, Program for Crystal Structure Refinement, University of Göttingen, Göttingen, Germany, **1997**.
- [37] C. M. MacNeill, C. S. Day, A. Marts, A. Lachgar, R. E. Noftle, *Inorg. Chim. Acta* **2011**, *365*, 196.
- [38] D. T. Tran, D. Chu, A. G. Oliver, S. R. J. Oliver, *Inorg. Chem. Commun.* **2010**, *13*, 649.
- [39] J. Zhou, S. H. Yan, D. Q. Yuan, X. J. Zheng, L. C. Li, L. P. Jin, *CrystEngComm* **2009**, *11*, 2640.
- [40] A. L. Spek, *PLATON*, Program for Single-crystal structure validation, *J. Appl. Crystallogr.* **2003**, *36*, 7.
- [41] A. Vishnyakov, P. I. Ravikovitch, A. V. Neimark, M. Bulow, O. M. Wang, *Nano Lett.* **2003**, *3*, 713.

Received: March 23, 2011

Published Online: June 6, 2011